

RSC Advances



This is an *Accepted Manuscript*, which has been through the Royal Society of Chemistry peer review process and has been accepted for publication.

Accepted Manuscripts are published online shortly after acceptance, before technical editing, formatting and proof reading. Using this free service, authors can make their results available to the community, in citable form, before we publish the edited article. This *Accepted Manuscript* will be replaced by the edited, formatted and paginated article as soon as this is available.

You can find more information about *Accepted Manuscripts* in the [Information for Authors](#).

Please note that technical editing may introduce minor changes to the text and/or graphics, which may alter content. The journal's standard [Terms & Conditions](#) and the [Ethical guidelines](#) still apply. In no event shall the Royal Society of Chemistry be held responsible for any errors or omissions in this *Accepted Manuscript* or any consequences arising from the use of any information it contains.

TiO₂ nanoparticle interactions with supported lipid membranes

– an example of removal of membrane patches

*Fang Zhao,¹ Jenny Perez Holmberg,² Zareen Abbas,² Rickard Frost,¹ Tora Sirkka,¹ Bengt Kasemo,¹
Martin Hassellöv,³ and Sofia Svedhem^{1,*}*

¹ Dept. of Applied Physics, Chalmers University of Technology, SE-412 96 Göteborg, Sweden

² Dept. of Chemistry and Molecular Biology, University of Gothenburg, SE-412 96 Göteborg, Sweden

³ Dept. of Marine Sciences, University of Gothenburg, SE-40530 Göteborg, Sweden

*sofia.svedhem@chalmers.se

ABSTRACT There is a need for different levels of model systems for effect studies of engineered nanoparticles and the development of nanoparticle structure-activity relationships in biological systems. Descriptors for nanoparticles based on their interactions in molecular model systems may become useful to predict toxicological responses of the nanoparticles in cells. Towards this end, we report on nanoparticle-induced formation of holes in supported model membranes. Specifically, TiO₂ nanoparticle - lipid membrane interactions were studied under low ionic strength, basic conditions (pH 8), using different membrane compositions and several surface-sensitive techniques. It was found that for mixed POPC/POPG (PG fractions $\geq 35\%$) membranes on silica supports, under conditions where electrostatic repulsion was expected, the addition of TiO₂ nanoparticles resulted in transient interaction curves, consistent with the removal of part of the lipid membrane. The formation of holes was inferred from quartz crystal microbalance with dissipation (QCM-D) monitoring, as well as from optical measurements by reflectometry, and also verified by atomic force microscopy (AFM) imaging. The interaction between the TiO₂ nanoparticles and the PG-containing membranes was dependent on the presence of Ca²⁺ ions. A mechanism is suggested where TiO₂ nanoparticles act as scavengers of Ca²⁺ ions associated with the supported membrane, leading to a weakening of the interaction between the membrane and the support and subsequent removal of lipid mass as TiO₂ nanoparticles spontaneously leave the surface. This mechanism is consistent with the observed formation of holes in the supported lipid membranes.

KEYWORDS lipid membrane, titanium dioxide, nanoparticle, electrostatic interaction, quartz crystal microbalance with dissipation monitoring

INTRODUCTION

Nanoparticles (NPs) receive increasing attraction due to their unique physicochemical properties and many fields of application, leading more recently to safety aspects related to potential adverse effects on human health and/or ecosystem.¹⁻³ NPs possess unique optical, magnetic, electrical and chemical properties different from their bulk states. This makes nanomaterials attractive candidates for a wide range of industrial products, including cosmetics, pharmaceuticals, catalysts, solar cells, construction materials, and biosensors. Most of the ongoing research in this area is focusing on properties and synthesis of nanosized materials, while less attention has been paid to the fundamental aspects of their interaction with biological systems. However, there is currently a growing concern about and attention to the latter effects. In fact, there is increasing evidence of specific effects of NPs on cells, and it is therefore of significant interest to understand the underlying mechanisms behind these observations.^{4,5} Specifically, it is of interest to establish structure-activity relationships for NP interactions in biological systems, where general nanoparticle surface properties such as charge and amphiphilicity are expected to be important, and further tuned by biospecific recognition.

Titanium oxide is a common material, often in the form of a nanomaterial, which is used in various applications due to its many attractive properties such as biocompatibility, photocatalysis, whiteness in paints, and charge carrier in solar cells. TiO₂ exists in three crystal structures, brookite, anatase and rutile. The rutile structure, or sometimes also amorphous TiO₂, is the more biocompatible form of TiO₂, whereas the anatase structure is the photo(catalytically) active one.^{6,7} Titanium implants are widely applied in medical implants owing to their outstanding ability for osseointegration.⁸⁻¹¹ A thin oxide layer is spontaneously formed on the titanium surface in air, and it is the titanium dioxide (TiO₂) layer which is responsible for the favorable interaction of titanium implants with tissues and bones.¹⁰ Titanium oxide is also a promising material for novel photovoltaic solar cells,^{7,12} especially for so called dye sensitized solar cells. By controlling the geometry of titanium oxide particles, especially in the nanodimension, their properties can be tuned. While rutile is thermodynamically favored for large particle sizes, anatase and brookite are energetically favored for small nanoparticle sizes.¹³

Motivated by the great value and variety of applications of TiO₂ NPs in biomedical and consumer products, both theoretical and experimental studies have been carried out to improve synthesis procedures and colloidal stability of particle suspensions.¹⁴⁻¹⁶ It is well known that the surface charge of TiO₂ NPs can be controlled through varying parameters such as size, shape, and the dispersing intermediate (importantly pH).¹⁷⁻²⁰ Despite the fact that the surface properties of TiO₂ NPs constitute an important research topic, only few studies have been performed addressing the interfacial interaction between TiO₂ NPs and lipid membranes. For example, the presence of calcium ions has been found to be important for the formation of some supported lipid bilayers on planar TiO₂ substrates.^{21, 22} One important motivation for similar studies is to understand the role of TiO₂ layers for the biocompatibility of titanium implants, as well as the potential toxicity of those metal oxide NPs to cells.²³⁻²⁶ Such results could also be important to understand effects of nanosized wear products which may form around implants.

Surface-supported lipid membranes are extensively studied as simplified model systems for the basic functions of biological membranes, such as lipid flip-flop,²⁷⁻²⁹ membrane pore formation,^{30, 31} functions of membrane proteins,^{32, 33} lipid transfer,³⁴ membrane fusion,³⁵ or viral infection.^{36, 37} These model membrane systems can be designed to address specific questions by varying the composition of lipid components and the choice of surface-analytical technique, to allow the investigation of the relation between structural properties and functional aspects of lipid membrane interactions. The dynamics of the supported lipid membrane platform is especially useful, e.g. in studies of tethered particles.³⁸

In the present study, we use supported lipid membranes as model systems to probe the interaction between TiO₂ NPs and lipid membranes by the quartz crystal microbalance with dissipation (QCM-D) technique. Similarly, we have previously used QCM-D to study structural rearrangements of drug carriers upon adsorption to lipid membrane surfaces.³⁹⁻⁴¹

QCM-D is an acoustic sensing method which measures mass uptake and structural properties of the mass adsorbed to the sensor surface. Here, the QCM-D results are validated by two other surface analytical techniques; reflectometry and atomic force microscopy (AFM). In particular the combination

of QCM-D and AFM is a powerful means to study these systems due to the different sensing principles. Phosphatidylglycerol (PG)-containing supported membranes have been used as a model for bacterial,^{42,}⁴³ as well as mammalian membranes.³¹ We focus on a comparison of the interaction of TiO₂ NPs with lipid membranes of different compositions, for a given buffer condition (low ionic strength, pH 8). Our study shows the expected accumulation of TiO₂ NPs on membranes under conditions for electrostatic attraction, but it also results in a mechanistic model for Ca²⁺-dependent removal of lipid mass from supported lipid membranes with a large enough fraction of PG lipids. This model is a contribution towards increased understanding of the interaction of TiO₂ NPs with cells, especially at the nanoscale, and the mechanisms behind effects on cells which might be associated with these interactions. The results lead us to discuss the relevance of supported lipid membranes for the development of structure-activity relationships.

RESULTS

The properties of the TiO₂ NP used in this study are described below, followed by the real-time nanoparticle – lipid membrane interaction results obtained by QCM-D and reflectometry, as well as AFM images of membranes subsequent to the exposure to nanoparticles.

TiO₂ NP properties. Stable suspensions of small, cationic TiO₂ NPs were synthesized at pH 2.5, following a protocol described elsewhere.⁴⁴ Here, the NP average size was 15 nm, and the size of the NPs increased to around 60 nm (Table 1) during a charge reversal step where the pH of the suspension was increased through the isoelectric point (pI ~ 5.5) by rapid addition of aqueous NaOH. The NP suspension was diluted in a 10 mM TRIS buffer of pH 8, and at this pH the zeta potential of the TiO₂ NPs was around -27 mV (Table 1). A low ionic strength buffer was used in the interaction experiments to avoid NP precipitation. It is noteworthy, that often during nanoparticle synthesis, a surface active compound is added which then remain at the surface of the nanoparticle. The TiO₂ NPs synthesized here, have a clean surface.

Table 1. Size and zeta potential of TiO₂ NPs and liposomes determined by DLS measurements.

Sample	Size (nm)	Polydispersity index	Zeta potential (mV)
TiO ₂ NPs (TRIS buffer)	57±1	0.2	-27±2
POPC liposomes (TRIS buffer)	84±3	0.1	-2±1
POPC/POEPC 1:1 liposomes (TRIS buffer)	94±1		+59±1
POPC/POPG 1:1 liposomes (TRIS buffer)	82±1		-47±1
POPC/POPG 1:1 liposomes (TRIS-CaCl ₂ buffer; 1 mM CaCl ₂)	79±1		-27±2
POPC/POPG 1:1 liposomes (TRIS-CaCl ₂ buffer; 2 mM CaCl ₂)	77±2		-22±1
POPC/POPG 1:1 liposomes (TRIS-CaCl ₂ buffer; 4 mM CaCl ₂)	80±1		-19±1
POPC/POPG 1:1 liposomes (TRIS-CaCl ₂ buffer; 8 mM CaCl ₂)	185±10	0.5	-14±1

The synthesis and stabilization of nanoparticles free from organic molecules are challenging tasks. In this particular study, additional experiments performed at a much later occasion showed similar but not identical results with respect to the particle size distribution. The particles synthesized at later stage had average particle diameter between 16 and 17 nm. Since synthesis method is based on hydrolysis of TiCl₄ a slight temperature variation can affect particle size. However, the particle suspensions at pH 2.5 were stable. Such a small variation in particle size does not have any effect on the particle surface charge density as shown in our previous study.¹⁸ Therefore we can safely conclude that such small particle size variation has negligible effect on the nanoparticle interaction with lipid membranes.

Formation of supported lipid membranes. Lipid membranes of different compositions were formed on SiO₂ supports by the well-established adsorption - spontaneous rupture – fusion process of adsorbed liposomes.⁴⁵ The properties of the liposomes used are summarized in Table 1. The average diameter of all liposomes of different compositions was similar (~80 nm), but their zeta potentials decreased with

the fraction of negatively charged POPG and increased with positively charged POEPC, which is consistent with our previous work.⁴⁶ In order to overcome the electrostatic repulsion between the negatively charged surface and negatively charged liposomes, calcium ions were added to the buffer when forming negatively charged supported lipid bilayers containing large fractions of PS or PG on SiO₂, according to published protocols.^{46, 47} The PDI for POPC/POPG in Tris buffer containing 8 mM CaCl₂ is a bit higher than the rest of investigated systems (Table 1). This is probably due the fact that hydrodynamic size determination by light scattering methods is very sensitive to the presence of aggregation. Even very few aggregates can increase PDI.

In the following, we will assume that the composition of each prepared supported lipid membrane formed is similar to that of the liposomes used for their formation (suggesting a symmetric distribution of lipids between the two leaflets, for details see discussion). Thus, the zeta potential of a particular supported lipid bilayer is assumed to be represented by the zeta potential of the corresponding liposomes. The lipid membranes formed (details on the lipid membrane formation process have been reported elsewhere^{46, 48}), resulted in QCM-D frequency and dissipation shifts of $\Delta f \sim -26$ Hz and $\Delta D < 0.5 \cdot 10^{-6}$, respectively, which are characteristic values for high quality lipid membranes formed with the actual method. An important feature of the QCM-D technique is its ability to characterize the viscoelastic properties of an adlayer formed on the sensor surface.⁴⁹ In particular, low ΔD values indicate the presence of only few or no remaining, intact liposomes on the surface.

TiO₂ NP interaction with POPC/POEPC lipid membranes. Figure 1A shows the typical QCM-D results when introducing TiO₂ NPs, at pH 8, to a lipid membrane with a high fraction of POEPC (POPC/POEPC 1:1). The frequency shift (Δf) decreases (corresponding to mass uptake) and the dissipation shift (ΔD) increases (corresponding to the formation of a more dissipative layer) upon addition of TiO₂ NPs. Under the present conditions, the frequency and dissipation shifts rapidly reach equilibrium (95% of the saturation value within minutes), and then stay constant upon rinsing, that is the

adsorption is irreversible on the time scale of the experiments. These data are consistent with the expected, electrostatically driven, adsorption of TiO₂ NPs to the membrane under the given conditions. On lipid membranes containing lower fractions of POEPC, the frequency shift (Δf) and the dissipation shift (ΔD) were both smaller, and decreased as a function of zeta potential for the corresponding liposome. These results are also expected. In the absence of the establishment of additional interactions in contact with the membrane, the adsorbed amount of TiO₂ NPs at equilibrium is expected to scale with the net charge of the lipid bilayer, since upon adsorption there is a competition between the attractive NP – lipid membrane and the NP – NP repulsive electrostatic interactions. No adsorption of TiO₂ NPs was observed onto lipid membranes with a fraction of POEPC below 10%. This indicates either that some force was needed to keep the NP bound to the membrane (e.g. due to thermal motions), or that EPC lipids are asymmetrically distributed between the two leaflets.

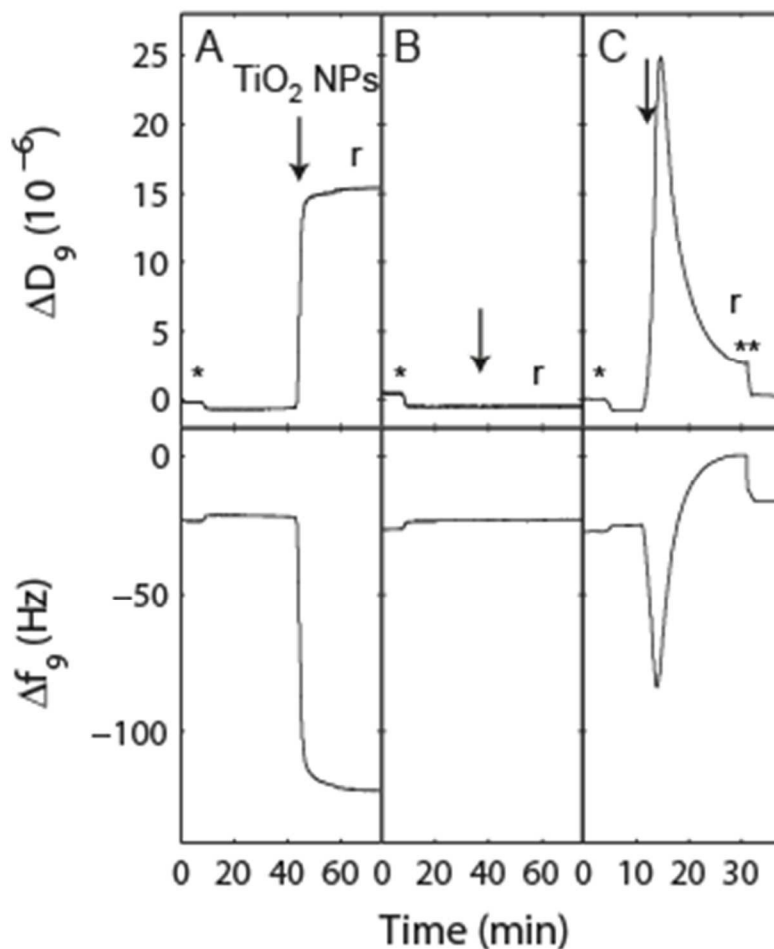


Figure 1 QCM-D frequency and dissipation shifts (Δf and ΔD , respectively) obtained when adding TiO₂ NPs (indicated by the arrows) at pH 8 (i.e. above the point of zero charge) to supported lipid bilayers of different composition; (A) POPC/POEPC 1:1 (positively charged), (B) POPC (neutral), and (C) POPC/POPG 1:1 (negatively charged). The lipid membrane formation occurred prior to the addition of TiO₂ particles and has been excluded from the graph. The membranes in A and B were formed in TRIS-NaCl, whereas the membrane in C was formed in TRIS-NaCl-CaCl₂. All membranes were rinsed with TRIS before and after (r) the addition of NPs diluted in TRIS. The buffer change caused the small shifts observed in the beginning of the experiment (indicated by *). In C, the buffer was changed back to TRIS-NaCl-CaCl₂ after the transient interaction with the NPs has reached equilibrium (indicated by **).

Additional experiments show that larger TiO₂ NPs (~200 nm, -34 mV) induce much higher dissipation shifts than smaller NPs for approximately the same frequency shift. This is a consequence of that larger NPs form more dissipative structures when adsorbed to the lipid membrane. Large dissipation shifts have also been observed when larger size lipid vesicles⁵⁰ or liposomes⁵¹ were adsorbed on TiO₂ or SiO₂ surfaces compared to smaller sized vesicles and liposomes.

The affinity of the NPs to the EPC-containing lipid membranes is in all cases strong, as seen by the non-reversibility of the QCM-D frequency and dissipation shifts upon rinsing. This was further confirmed in additional experiments where the NPs were added at lower concentration. These experiments showed that the lower the NP concentration, the longer time was needed to reach equilibration, whereas the final frequency and dissipation shifts did not differ a lot, and the NPs were irreversibly adsorbed while rinsing. Thus, the equilibrium of the interaction between the NP and the positively charged lipid membrane is strongly shifted towards adsorption of NPs for fractions of POEPC > 10% in the liposomes. A likely explanation for the high affinity of the TiO₂ NPs for the positively charged membrane, in view of the high mobility of lipids in the bilayer, is rearrangement of the charged lipids in the membrane, leading to accumulation of the oppositely charged lipid molecule in the membrane close to and underneath the NPs.⁴⁶

TiO₂ NP interaction with POPC, POPC/POPS and POPC/POPG lipid membranes. For lipid membranes formed from POPC, POPC/POPS and POPC/POPG mixtures (with a fraction of the anionic lipid < 25%), no adsorption of TiO₂ NPs to the corresponding membrane was observed, as exemplified in Figure 1B and as expected given the measured zeta potentials. In contrast, and counterintuitive for the measured zeta potentials, the addition of TiO₂ NPs to lipid membranes formed from liposomes containing a larger fraction of POPG (POPG fractions ≥ 35%) was quite different, as shown in Figure 1C (POPC/POPG 1:1). In these experiments, the QCM-D frequency shift (Δf) first decreased (indicating mass uptake), then increased (indicating mass loss), and gradually returned close to its original value, while the corresponding dissipation shift (ΔD) exhibited an opposite behavior with a maximum in the

signal, in time close to the frequency minimum. The interaction between the membrane and the TiO₂ NPs was studied in TRIS buffer, and upon changing the buffer back to TRIS-NaCl-CaCl₂ (which was used to form the supported membrane prior to the addition of NPs), the ΔD value could be compared to the baseline value before the addition of the TiO₂ NPs, but with a small increase of the Δf value (from -27 Hz to -23 Hz). This buffer change was performed to compensate for the (unusual and) large dissipation shifts for PG-containing supported lipid membranes in response to buffer changes when switching between a Ca²⁺ containing and a non-Ca²⁺ containing buffer.⁴⁷ Thus, when taking the buffer effect into consideration, the net result of the transient interaction curve obtained when the TiO₂ NPs were added to the POPC/POPG 1:1 membrane is a small decrease in mass compared to the mass of the lipid membrane before addition of the NPs. As shown in Figure 2, additional mass loss was observed when repeating again the TiO₂ NP addition and the same sequence of buffer changes. For each cycle, more mass was lost until two thirds of the lipid membrane mass was removed from the sensor surface (Figure 3). We associate this saturation effect with removal of all or most of the PG lipids from the membrane (see below). At this point, more POPC/POPG vesicles could be added to restore the membrane mass to its initial value (i.e. frequency and dissipation shifts corresponding the initial lipid membrane were regained, i.e. $\Delta f \sim -26$ Hz and $\Delta D < 0.5 \cdot 10^{-6}$). The restored membrane again interacted transiently with TiO₂ NPs (Figure 2, last part), causing mass loss.

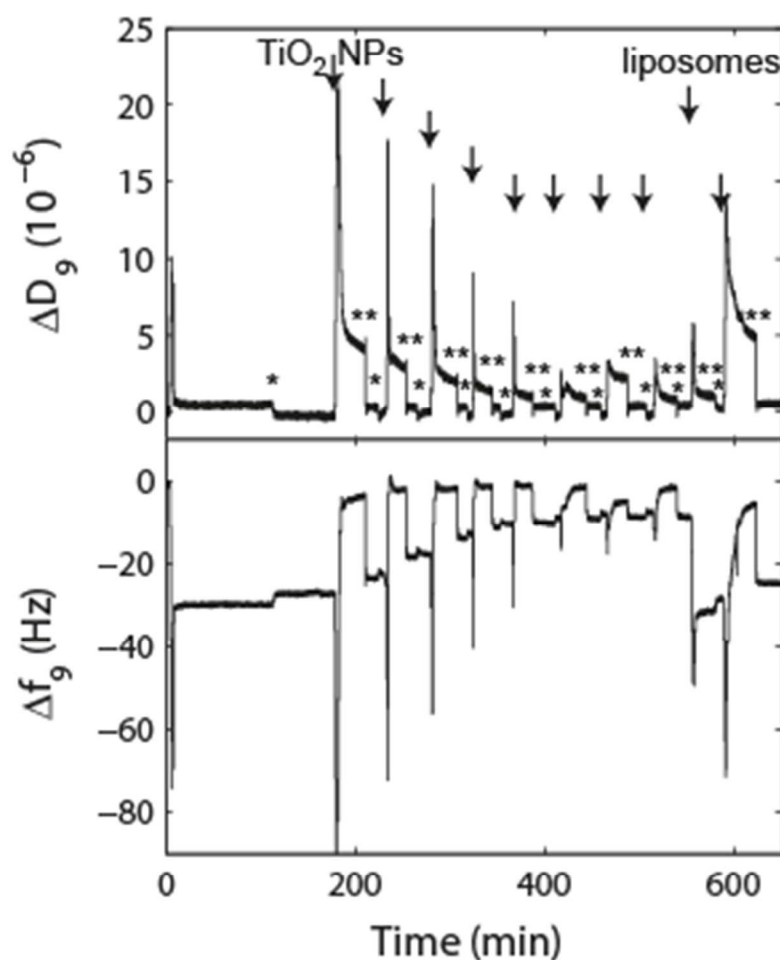


Figure 2 QCM-D frequency and dissipation shifts (Δf and ΔD , respectively) obtained when adding repeatedly TiO_2 NPs at pH 8 to a supported lipid membrane composed of POPC/POPG 1:1 (negatively charged). The lipid membrane formation at the beginning of the experiment (in TRIS-NaCl-CaCl₂) is followed by a buffer change to TRIS (indicated by *) and nine sequential additions of TiO_2 NPs in TRIS and buffer changes to TRIS-NaCl-CaCl₂ (indicated by **). At $t \sim 580$ min, more liposomes are added, before repeating one last time the TiO_2 addition.

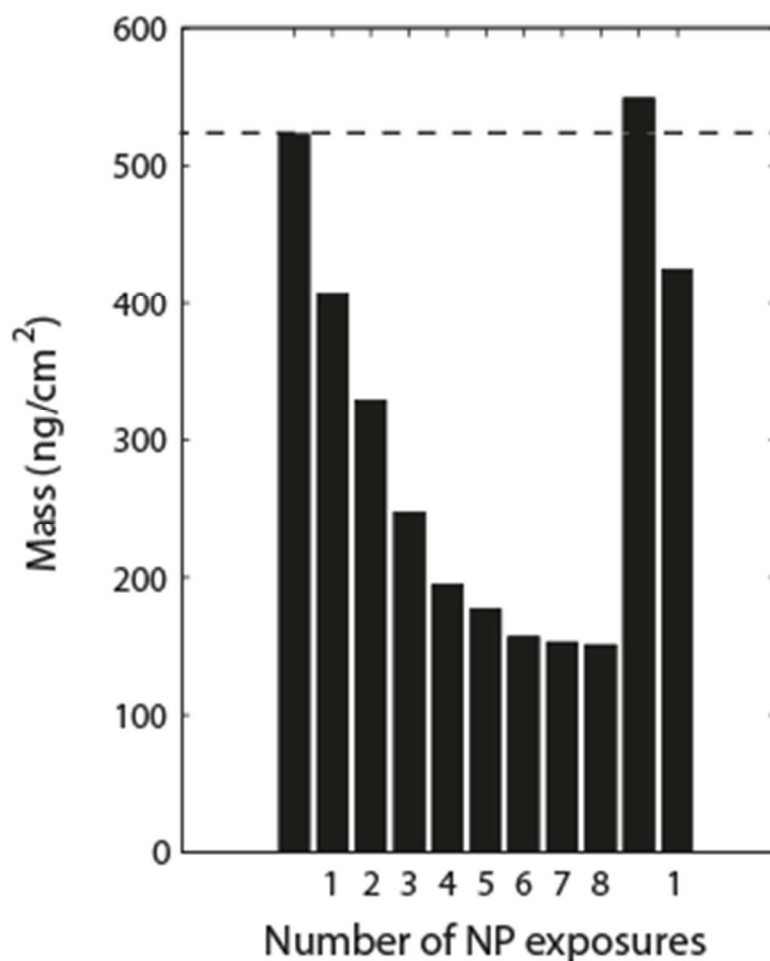


Figure 3 Lipid mass on the sensor surface at the different stages of the experiment shown in Figure 2, as modeled from the QCM-D data in Figure 2 using the Sauerbrey relationship. The changes in bar heights represent loss or gain of membrane mass. The bars 1-8 represent repeated exposures of the lipid membrane to TiO₂ NPs, causing a monotonous loss of lipid mass. Next, the lipid membrane mass increases due to re-addition of liposomes. The last bar represents the mass after the freshly repaired lipid membrane was once again exposed to TiO₂ NPs.

The remaining lipid membrane mass after each transient interaction with TiO₂ NPs is shown in Figure 3. The mass loss after each addition of TiO₂ NPs gradually decreases and eventually levels off after 8 additions of NPs and buffer changes. In other words TiO₂ NPs appear to remove, in each cycle, lipid material from the substrate, leaving holes in the membrane. Note that the maximum mass uptake of

TiO₂ NPs also decreases for each successive cycle (Figure 2, peak value of Δf), indicating that the fraction of POPG in remaining lipid patches decreases for each cycle, until the attraction between the membrane and the TiO₂ NPs can no longer be restored by supplying Ca²⁺ ions. In other words, it appears that the TiO₂ NP exposure cause selective removal of PG lipids. Mass loss is consistent with complementary combined QCM-D and reflectometry measurements where the QCM-D experiment and the optical measurement are performed at the same time and on the same lipid membrane. These experiments show the removal of lipid material for each additional cycle of addition of TiO₂ NP and Ca²⁺ ion addition to the PG-containing membranes (Supporting information Figure S1).

Imaging of the supported membranes by AFM. As suspected based on the data collected by QCM-D and by reflectometry, liquid phase AFM images of POPC:POPG (1:1) supported membranes which had been exposed to TiO₂ NPs revealed holes in the membrane. After two exposures to NPs, membrane defects of various sizes (hundreds of nm to several μm) were observed and holes were sparsely distributed. In Figure 4A, one large hole is shown. The surrounding membrane was detected by force spectroscopy where the presence of a lipid membrane is revealed by a step in the resulting force spectra during the approach (Figure 4B). This step was absent in the areas without a lipid membrane, *i.e.* in the holes. The height profile across a hole revealed a step of about 5 nm, a result that is in good agreement with the thickness of a lipid membrane (Figure 4C).

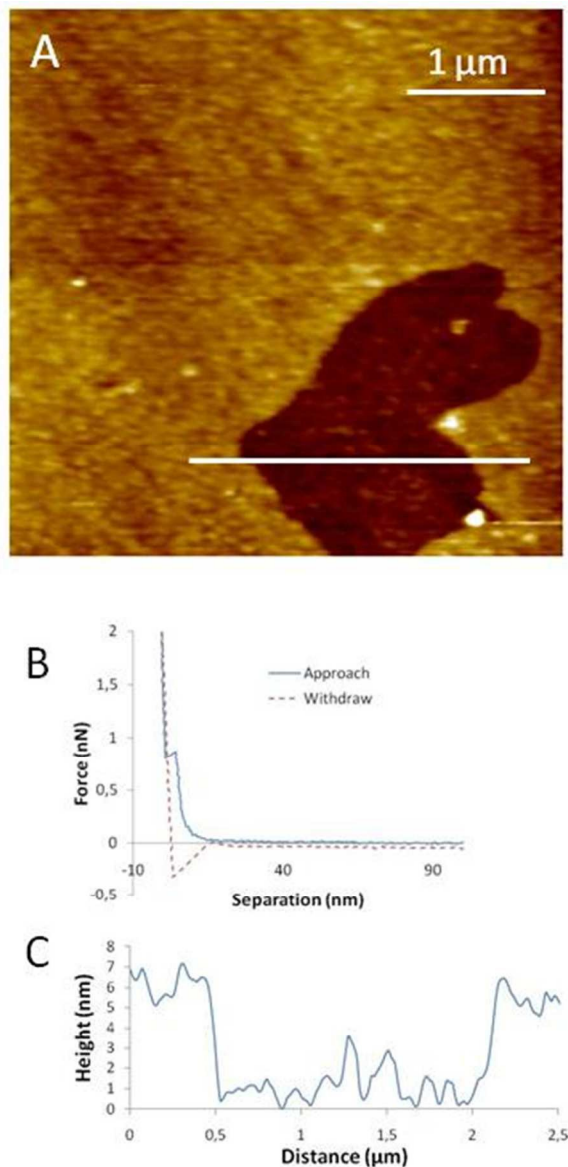


Figure 4 AFM data showing a hole in a POPC-POPG (1:1) lipid membrane induced by TiO₂ NPs. (A) AFM image of a micrometer sized hole in the lipid bilayer (z-range 20.9 nm). (B) Force curve detecting the presence of the lipid bilayer surrounding the hole. (C) Height profile across a hole according to the white line in (A). Note that the QCM-D sensor surface is fairly rough (The RMS value is 1.16 ± 0.08 nm according to specifications).

It would have been interesting to image as well the structure of a layer of TiO₂ NPs bound to POPC/POEPC supported membranes. However, it was not possible to image the adsorbed NPs in contact mode.

RSC Advances Accepted Manuscript

DISCUSSION

It is well known that divalent ions can strongly bind to the phosphoesters in the head group of phospholipids,^{22, 52} as well as to the surface of metal dioxides. In fact, Ca^{2+} ions have a much higher affinity for TiO_2 compared to SiO_2 , as evidenced by a huge difference in Ca^{2+} complexation constants (pKa 0.58-1.58 for rutile TiO_2 ⁵³ compared to pKa 6.9 for SiO_2 ⁵⁴). We therefore hypothesize that the observed attractive interaction between the PG-containing membranes and TiO_2 is mediated by Ca^{2+} ions associated with the lipid membrane on the SiO_2 surface, remaining there after the bilayer formation process in a Ca^{2+} -containing buffer. Note that when the buffer was changed from TRIS-NaCl- CaCl_2 to TRIS only, most of the salts (mainly NaCl) will be rinsed away, however, Ca^{2+} ions which have stronger affinity compared to Na^+ ions may still bind to POPG lipids head groups under low ionic strength conditions.⁵² In a previous study, we showed that a buffer change between TRIS-NaCl- CaCl_2 and TRIS-NaCl greatly affected the QCM-D characteristic of a similar PG-membrane, interpreted as replacement of Ca^{2+} ions bridging between the lipid membrane and the surface by Na^+ ions leading to a much weaker interaction between the lipid membrane and the surface.⁴⁷

Comparison between the expected and the observed result in interaction between the TiO_2 NPs and the POPC/POEPC lipid membranes

The large responses which were obtained by QCM-D for TiO_2 NPs interacting with the POPC/POEPC membranes were expected under the present experimental conditions. An attractive interaction potential was also obtained by DLVO calculations (as described in the Supporting information). The interactions were irreversible and the relative dissipation ($\Delta D/\Delta f$) quite low, both indicative of a firm interaction between the NPs and the lipid membrane.

Under repulsive conditions, NPs did not bind to the lipid membrane (i.e. < 30% of POPS or POPG), except for a high enough fraction (> 35%) of POPG. This latter result was unexpected (see also the DLVO calculations in the Supporting information). One explanation to this unexpected result would be

that, in this case, the zeta potential that we measure for the POPC/POPG liposomes does not serve as an appropriate estimate for the zeta potential of the POPC/POPG membranes formed onto the silica support. Unfortunately, we have not been able to experimentally measure the zeta potential of the supported membranes due to instrumental limitations. It is perhaps not unlikely that Ca^{2+} ions (included in the buffer during the formation of the supported lipid membrane) associate to the PG head groups in the upper lipid leaflet such that the zeta potential is reversed. This would then explain why an attractive interaction potential is obtained (see also the DLVO calculations in the Supporting Information). Alternatively, Ca^{2+} ions are present at the interface between the silica substrate and the lower leaflet of the POPC/POPG membrane, and the displacement of the ions to the upper leaflet occurs only as the TiO_2 NPs approach. Meanwhile, the repulsion between SiO_2 crystal and POPG lipids become stronger in the absence of Ca^{2+} ions.⁴⁷ This may explain why TiO_2 NPs remove lipid patches rather than remain immobilized onto the lipid membrane.

Role of Ca^{2+} ions for the removal of membrane caused by TiO_2 NPs. In control experiments, the addition of EDTA to a lipid bilayer composed of POPC/POPG (1:1) showed a similar behavior as TiO_2 NPs (Supporting Information, Figure S2), although without any removal of lipid material, which supports the role of the TiO_2 NPs as Ca^{2+} ion scavengers in our system. Repeated supply of calcium ions is necessary for the repeated removal of lipid material from the surface mediated by TiO_2 NPs (Figure 2 and Figure 3), further indicating the role of Ca^{2+} ions. Thus, based on our results, we propose the following mechanistic model for the formation of holes in POPC/POPG (> 35% PG) model membranes upon addition of TiO_2 NPs (Figure 5): (i) in the first step, a good quality POPC/POPG (1:1) supported membrane is formed in TRIS-NaCl- CaCl_2 buffer, followed by (ii) rinsing of the supported lipid membrane with the low ionic strength TRIS buffer. During this rinsing step, Ca^{2+} ions are retained by the lipid head groups in the lower lipid leaflet, due to a strong interaction between the lipid membrane and the silica surface (this will not happen in a high ionic strength buffer, where the electrostatic attraction is screened⁴⁷). We suggest that the retained Ca^{2+} ions are removed when (iii) adding TiO_2 NPs,

due to the high affinity between the TiO₂ NPs and the Ca²⁺ ions.⁵³ During this process, some lipids bind to the NPs and are removed by as the NP leave the surface under flow mode. After the removal of Ca²⁺ ions the interaction between the SiO₂ support and the remaining membrane is much weakened, until (iv) upon changing the buffer back to TRIS-NaCl-CaCl₂ which re-establish the tight binding of the lipid membrane to the silica surface. At this point the loss of lipid material can be observed by AFM as holes in the membrane.

We cannot distinguish between the scenario where the substrate has an important role for the retention of Ca²⁺ ions, and a situation where the binding of Ca²⁺ ions to the lipid membrane head groups alone will explain the observed interactions. This issue can be further addressed in molecular dynamics (MD) simulations. MD simulations between PS-containing membranes and TiO₂ substrates have previously suggested direct coordination of the phosphate or carbonyl oxygen atoms of PS and PC lipids with titanium sites.⁵⁵ In particular, we foresee that it will be possible to elaborate on the role of hydrogen bonding between the lipid head groups and the Ca²⁺ ions by comparing MD and further experimental results. We note that previous studies of thermodynamic driving forces for lipid flip-flop in supported membranes have revealed large opposing enthalpic and entropic contributions to the free energy, thus providing new perspectives on the energetics of membrane processes.^{56,57}

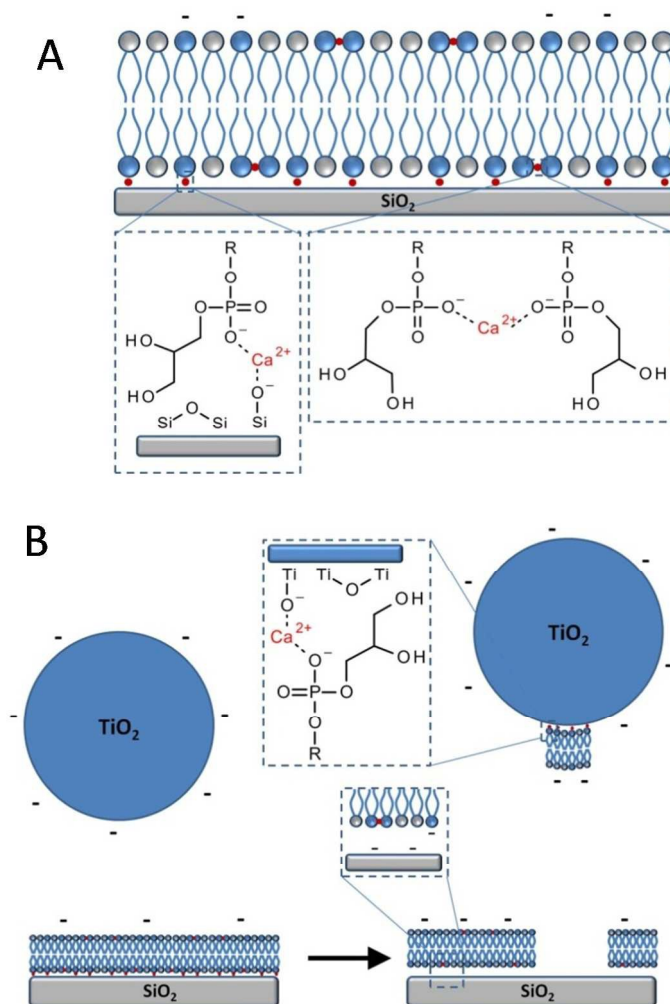


Figure 5 Schematic drawing describing the Ca^{2+} mediated process by which holes are formed in a POPG/POPC membrane interacting with TiO_2 NPs. In A, a plausible structure where POPG lipids in the POPC/POPG membrane are preferentially oriented towards the substrate is shown, where Ca^{2+} are predominantly bound to the interface between the membrane and the substrate. In B, it is inferred that Ca^{2+} in the presence of TiO_2 NPs preferentially accumulate at the lipid membrane TiO_2 interface, leading to removal of Ca^{2+} ions from the solid interface, and whole membrane patches from the SiO_2 substrate.

Nanoparticle descriptors in structure-activity relationships.

Functional descriptors for nanoparticles based on their interactions in molecular model systems may become useful to predict toxicological responses of the nanoparticles in cells. Such a development will require the identification of biologically relevant molecular assemblies which can be associated with nanotoxicological mechanisms. The further exploring of the supported lipid membrane platform might be useful towards this end, adding to, e.g., studies of antibacterial agents⁴³ and peptide translocation studies³¹. The POPC/POPG (1:1) supported membranes may serve to experimentally probe for nanoparticles which act as scavengers of cations, a property which is likely governed by the pKa of functional groups at the surface of the nanoparticle along with the number of charged sites per surface area. For the case of TiO₂, the density of charged sites on the surface of the oxide is much higher compared to the bilayer on average, which drives the preferential binding of Ca²⁺ to the TiO₂ surface,²⁴ leading to, in our model system, removal of lipid mass and the formation of holes in the supported membrane. Since TiO₂ is biocompatible, this may be a physicochemical function which can be correlated to beneficial biological responses.

The role of Ca²⁺ ions in biomolecular adsorption to metal oxides has also been observed for adsorption of human albumin on TiO₂ surface.⁵⁸ Under physiologic conditions (i.e. pH 7), negatively charged albumin can bind to negatively charged TiO₂ surface via Ca²⁺ ions, which is in analogous with our studies of POPG lipids. The way nanoparticles interact with selected proteins (or other biomolecules) is likely a good complement to the experiments with supported membranes in the search for useful structure-activity relationships.

Conclusion

In conclusion, we have shown, by a combination of several surface sensitive analytical techniques, that TiO₂ NPs induce holes in PG-containing supported lipid membranes via a Ca²⁺ dependent mechanism. We suggest that this process is driven by the strong affinity between Ca²⁺ ions and TiO₂, and that Ca²⁺ ions are displaced, by approaching NPs, from the interface between the lipid membrane and the silica support to the interface between the lipid membrane and the TiO₂ NPs. Due to the weakening of the interaction between the lipid membrane and the silica support, lipid mass is removed along with TiO₂ NPs diffusing away from the surface.

MATERIALS AND METHODS

Unless otherwise stated, chemicals were obtained from commercial sources and used without further purification. The lipids 1-palmitoyl-2-oleoyl-*sn*-glycero-3-phosphocholine (POPC), 1-palmitoyl-2-oleoyl-*sn*-glycero-3-phospho-(1'-*rac*-glycerol) (POPG), 1-palmitoyl-2-oleoyl-*sn*-glycero-3-[phospho-L-serine] (POPS), and 1-palmitoyl-2-oleoyl-*sn*-glycero-3-ethylphosphocholine (POEPC) were obtained from Avanti Polar Lipids Inc., USA. Water was deionized (resistivity > 18 M Ω /cm) and purified using a MilliQ plus unit (Millipore, France). All buffers were filtered and degassed before use. The following buffers were used throughout this study: TRIS (10 mM TRIS, pH 8), TRIS-NaCl (10 mM TRIS, 100 mM NaCl, pH 8), TRIS-NaCl-CaCl₂ (10 mM TRIS, 100 mM NaCl, 10 mM CaCl₂, pH 8), and TRIS-CaCl₂. (10 mM TRIS, pH 8, with CaCl₂ added at a given concentration).

TiO₂ NP synthesis and characterization. TiO₂ NPs were prepared by means of a low-temperature synthetic route based on the hydrolysis of TiCl₄ in water, following a published procedure.⁴⁴ The initial synthesis product was dialyzed to pH 2.5. The primary particle size was 15 nm. The TiO₂ suspension was subjected to charge reversal by increasing the pH of the solution by rapid addition of 1 M NaOH to the aqueous NP solution, followed by mixing. The resulting pH was between 11 and 12. This led to some agglomeration and increase in size (DLS size increased to 50-60 nm. Prior to QCM-D analysis of the TiO₂ NP- SLB interactions, the NPs were diluted in TRIS which resulted in some additional agglomeration, though not on the timescale of the experiment.

Liposome preparation. Phospholipid mixtures of desired compositions were dissolved in chloroform. Lipid mixtures were dried under a gentle flow of N₂ to prepare a lipid film on the walls of round-bottom flasks, and solvent residuals were removed under reduced pressure. The lipid films were hydrated in TRIS-NaCl buffer. The lipid suspensions were extruded 11 times each through 100 nm and 30 nm polycarbonate membranes. The resulting vesicle solutions were refrigerated under N₂. Liposomes prepared in this way were characterized with respect to size and zeta potential by dynamic light scattering and electrodynamic mobility, respectively.⁴²

Dynamic light scattering and electrodynamic mobility. The average hydrodynamic radius and the zeta potential of TiO₂ NPs and liposomes were determined in a Malvern Zetasizer Nano ZS (Malvern Instr., UK). Vesicles were diluted in TRIS-NaCl buffer to a final concentration of 0.1 mg/mL. TiO₂ NPs were diluted in TRIS to a final concentration of 0.1 mg/mL. Statistics are given as means and standard variations of three replicates.

QCM-D Measurements. QCM-D measurements were performed in flow mode using a Q-Sense E4 instrument (Q-Sense AB, Sweden). AT-cut quartz crystals with a fundamental frequency of 5 MHz coated with SiO₂ were purchased from Q-Sense AB. In principle, a quartz crystal is excited to oscillate in the thickness shear mode at its fundamental resonant frequency (f_0) by applying across the crystal an RF voltage near its resonant frequency. The adsorption of material on top of the crystal results in a decrease in resonant frequency (Δf) related to the corresponding mass change (Δm). The energy dissipation factor (D), which shows the viscoelastic properties of adsorbed film, can be obtained by interrupting the driving voltage and measuring the decay time of the induced oscillation.⁵⁹ The presented data were measured at the ninth overtone ($n = 9$) and normalized to the fundamental frequency by dividing by 9. Prior to the experiment, the crystals were cleaned in 10 mM sodium dodecyl sulfate solution, rinsed thoroughly with water, dried under N₂, and treated with UV/ozone for 3 × 15 min with rinsing and drying in between. The measurements were carried out at 22 °C at a flow rate of 100 μ L/min. Lipid membranes of different composition were formed on the cleaned SiO₂ supports. Vesicles were diluted in buffer to a final concentration of 0.1 mg/mL to form bilayer. Note that TRIS-NaCl was used for membranes containing the positively charged POEPC lipid, whereas TRIS-NaCl-CaCl₂ was used for membranes containing neutral or negatively charged lipids. TiO₂ NPs were diluted in TRIS to a final concentration of 0.1 mg/mL. Control experiments were performed where care was taken to avoid that TiO₂ NPs were exposed to light.

AFM measurements. AFM imaging was carried out using a PicoSPM microscope (Agilent/Molecular Imaging Inc., Palo Alto, CA) and MSCT-AUNM MicroLever silicon nitride tips (Veeco Europe, Dourdan, France). The cantilevers used have a spring constant of 30 pN/nm and the tips a radius of

curvature < 20 nm (according to specifications). Images were recorded using scan speeds in the range 1.5-2.0 lines/s. The experiments were performed using constant-force contact mode with low imaging force. The fluid cell consisted of an O-ring pressed against the substrate (UV-ozone treated SiO₂-coated QCM-D crystal) with a customized holder. The fluid cell contained 300 μ L of liquid during imaging and all liquid exchanges were made by repeatedly adding and withdrawing 300 μ L of liquid. Initially, a POPC:POPG (1:1) supported lipid membrane was formed on the crystal in TRIS-NaCl-CaCl₂. After formation of the lipid membrane, the buffer was exchanged to TRIS. As a next step, the TiO₂ NPs were added and were left to incubate for 5 min. Subsequently, the surface was rinsed with TRIS before changing the buffer to TRIS-NaCl-CaCl₂. Before imaging the surface, two cycles of NP addition were made and the buffer was changed back to TRIS. Images were treated and analyzed using the SPIP software version 3.0.0.9 (Image Metrology Inc., Ljungby, Denmark). Force spectroscopy experiments were performed with a constant approach/retraction speed of $v = 280$ - 560 nm/s, corresponding to a force loading rate $vk = 8.40$ - 16.8 nN/s. Deflection-position raw data were converted to force-distance curves with SPIP software using specified values for the cantilever spring constant.

ACKNOWLEDGMENT This research was carried out within the project NanoSphere funded by Swedish Environmental Research Council FORMAS. Additional financial support was obtained from the Swedish Research Council (project numbers 621-2007-4375 and 2012-4217). Julian Gallego is acknowledged for help with the TiO₂ NP charge reversal procedure.

SUPPORTING INFORMATION. Additional QCM-D, reflectometry and DLVO results are available as Supporting Information.

REFERENCES

1. P. Rivera Gil, G. Oberdorster, A. Elder, V. Puentes and W. J. Parak, *Acs Nano*, 2010, **4**, 5527-5531.
2. S. M. Moghimi, D. Peer and R. Langer, *Acs Nano*, 2011, **5**, 8454-8458.
3. C. R. Thomas, S. George, A. M. Horst, Z. X. Ji, R. J. Miller, J. R. Peralta-Videa, T. A. Xia, S. Pokhrel, L. Madler, J. L. Gardea-Torresdey, P. A. Holden, A. A. Keller, H. S. Lenihan, A. E. Nel and J. I. Zink, *Acs Nano*, 2011, **5**, 13-20.
4. A. E. Nel, L. Madler, D. Velegol, T. Xia, E. M. V. Hoek, P. Somasundaran, F. Klaessig, V. Castranova and M. Thompson, *Nat Mater*, 2009, **8**, 543-557.
5. J. Kim, S. V. Chankeshwara, F. Thielbeer, J. Jeong, K. Donaldson, M. Bradley and W.-S. Cho, *Nanotoxicology*, 2015, DOI: 10.3109/17435390.2015.1022887, 1-8.
6. T. Kubo, H. Orita and H. Nozoye, *J. Am. Chem. Soc.*, 2007, **129**, 10474-10478.
7. A. Wold, *Chem. Mater.*, 1993, **5**, 280-283.
8. J. E. Ellingsen, *Biomaterials*, 1991, **12**, 593-596.
9. X. J. Khoo, P. Hamilton, G. A. O'Toole, B. D. Snyder, D. J. Kenan and M. W. Grinstaff, *J Am Chem Soc*, 2009, **131**, 10992-10997.
10. J. Michael, L. Schönzart, I. Israel, R. Beutner, D. Scharnweber, H. Worch, U. Hempel and B. Schwenzer, *Bioconjugate Chem.*, 2009, **20**, 710-718.
11. J. G. Morales, R. R. Clemente, B. Armas, C. Combescure, R. Berjoan, J. Cubo, E. Martinez, J. G. Carmona, S. Garelik, J. Murtra and D. N. Muraviev, *Langmuir*, 2004, **20**, 5174-5178.
12. M. Pastore and F. De Angelis, *Acs Nano*, 2010, **4**, 556-562.
13. M. R. Ranade, A. Navrotsky, H. Z. Zhang, J. F. Banfield, S. H. Elder, A. Zaban, P. H. Borse, S. K. Kulkarni, G. S. Doran and H. J. Whitfield, *Proceedings of the National Academy of Sciences of the United States of America*, 2002, **99**, 6476-6481.
14. M. Anpo, T. Shima, S. Kodama and Y. Kubokawa, *J. Phys. Chem.*, 1987, **91**, 4305-4310.
15. C. Kormann, D. W. Bahnemann and M. R. Hoffmann, *J. Phys. Chem.*, 1988, **92**, 5196-5201.
16. N. Serpone, D. Lawless and R. Khairutdinov, *J. Phys. Chem.*, 1995, **99**, 16646-16654.
17. Z. Abbas, C. Labbez, S. Nordholm and E. Ahlberg, *J Phys Chem C*, 2008, **112**, 5715-5723.
18. J. P. Holmberg, E. Ahlberg, J. Bergenholtz, M. Hasselov and Z. Abbas, *J Colloid Interf Sci*, 2013, **407**, 168-176.
19. M. D. Chadwick, J. W. Goodwin, E. J. Lawson, P. D. A. Mills and B. Vincent, *Colloid Surface A*, 2002, **203**, 229-236.
20. B. Vincent, Z. Kiraly, S. Emmett and A. Beaver, *Colloid Surface*, 1990, **49**, 121-132.
21. F. F. Rossetti, M. Bally, R. Michel, M. Textor and I. Reviakine, *Langmuir*, 2005, **21**, 6443-6450.
22. F. F. Rossetti, M. Textor and I. Reviakine, *Langmuir*, 2006, **22**, 3467-3473.
23. J. R. Gurr, A. S. S. Wang, C. H. Chen and K. Y. Jan, *Toxicology*, 2005, **213**, 66-73.
24. M. Horie, K. Nishio, K. Fujita, S. Endoh, A. Miyauchi, Y. Saito, H. Iwahashi, K. Yamamoto, H. Murayama, H. Nakano, N. Nanashima, E. Niki and Y. Yoshida, *Chemical Research in Toxicology*, 2009, **22**, 543-553.
25. C. M. Sayes, R. Wahi, P. A. Kurian, Y. P. Liu, J. L. West, K. D. Ausman, D. B. Warheit and V. L. Colvin, *Toxicol Sci*, 2006, **92**, 174-185.
26. T. Xia, M. Kovoichich, M. Liong, L. Madler, B. Gilbert, H. B. Shi, J. I. Yeh, J. I. Zink and A. E. Nel, *Acs Nano*, 2008, **2**, 2121-2134.
27. J. Liu and J. C. Conboy, *J Am Chem Soc*, 2004, **126**, 8376-8377.
28. Y. J. Jing, H. D. Trefna, M. Persson and S. Svedhem, *Bba-Biomembranes*, 2015, **1848**, 1417-1423.
29. Y. Gerelli, L. Porcar, L. Lombardi and G. Fragneto, *Langmuir*, 2013, **29**, 12762-12769.
30. E. Briand, M. Zach, S. Svedhem, B. Kasemo and S. Petronis, *Analyst*, 2010, **135**, 343-350.

31. S. Piantavigna, M. E. Abdelhamid, C. Zhao, X. H. Qu, G. A. McCubbin, B. Graham, L. Spiccia, A. P. O'Mullane and L. L. Martin, *Chempluschem*, 2015, **80**, 83-90.
32. I. Carton, A. R. Brisson and R. P. Richter, *Anal. Chem.*, 2010, **82**, 9275-9281.
33. H. Pace, L. S. Nystrom, A. Gunnarsson, E. Eck, C. Monson, S. Geschwindner, A. Snijder and F. Hook, *Anal. Chem.*, 2015, **87**, 9194-9203.
34. A. Wikstrom, S. Svedhem, M. Sivignon and B. Kasemo, *Journal of Physical Chemistry B*, 2008, **112**, 14069-14074.
35. L. Simonsson, P. Jönsson, G. Stengel and F. Höök, *Chemphyschem*, 2011, **11**, 1011-1017.
36. M. Fischlechner, U. Reibetanz, M. Zaulig, D. Enderlein, J. Romanova, S. Leporatti, S. Moya and E. Donath, *Nano Lett.*, 2007, **7**, 3540-3546.
37. G. E. Rydell, A. B. Dahlin, F. Höök and G. Larson, *Glycobiology*, 2009, **19**, 1176-1184.
38. K. L. Hartman, S. Kim, K. Kim and J. M. Nam, *Nanoscale*, 2015, **7**, 66-76.
39. C. C. Frost, R.; Gradfil, B.; Kasemo, B.; Svedhem, S., *Journal of Biomaterials and Nanobiotechnology*, 2011, **2**, 181-193.
40. R. Frost, G. Coue, J. F. Engbersen, M. Zach, B. Kasemo and S. Svedhem, *J Colloid Interface Sci*, 2011, **362**, 575-583.
41. E. Rascol, J. M. Devoisselle and J. Chopineau, *Nanoscale*, 2016, **8**, 4780-4798.
42. A. Mechler, S. Praporski, K. Atmuri, M. Boland, F. Separovic and L. L. Martin, *Biophys J*, 2007, **93**, 3907-3916.
43. T. Joshi, Z. X. Voo, B. Graham, L. Spiccia and L. L. Martin, *Biochimica Et Biophysica Acta-Biomembranes*, 2015, **1848**, 385-391.
44. Z. Abbas, J. Perez Holmberg, A.-K. Hellström, M. Hagström, J. Bergenholtz, M. Hassellöv and E. Ahlberg, *Colloids Surf. Physicochem. Eng. Aspects*, 2011, **384**, 254-261.
45. R. P. Richter, R. Bérat and A. R. Brisson, *Langmuir*, 2006, **22**, 3497-3505.
46. A. Kunze, S. Svedhem and B. Kasemo, *Langmuir*, 2009, **25**, 5146-5158.
47. A. Kunze, F. Zhao, A. K. Marel, S. Svedhem and B. Kasemo, *Soft Matter*, 2011, **7**, 8582.
48. C. A. Keller and B. Kasemo, *Biophys J*, 1998, **75**, 1397-1402.
49. M. Rodahl, F. Hook and B. Kasemo, *Anal Chem*, 1996, **68**, 2219-2227.
50. E. Reimhult, F. Hook and B. Kasemo, *J Chem Phys*, 2002, **117**, 7401-7404.
51. Y. J. Jing, H. Trefna, M. Persson, B. Kasemo and S. Svedhem, *Soft Matter*, 2014, **10**, 187-195.
52. P. M. Macdonald and J. Seelig, *Biochemistry*, 1987, **26**, 1231-1240.
53. M. K. Ridley, T. Hiemstra, W. H. van Riemsdijk and M. L. Machesky, *Geochim Cosmochim Ac*, 2009, **73**, 1841-1856.
54. M. Berka and I. Banyai, *J. Colloid Interface Sci.*, 2001, **233**, 131-135.
55. A. Fortunelli and S. Monti, *Langmuir*, 2008, **24**, 10145-10154.
56. T. C. Anglin, M. P. Cooper, H. Li, K. Chandler and J. C. Conboy, *J Phys Chem B*, 2010, **114**, 1903-1914.
57. K. L. Brown and J. C. Conboy, *J Phys Chem B*, 2015, **119**, 10252-10260.
58. A. Klinger, D. Steinberg, D. Kohavi and M. N. Sela, *J Biomed Mater Res*, 1997, **36**, 387-392.
59. M. Rodahl and B. Kasemo, *Rev Sci Instrum*, 1996, **67**, 3238-3241.

SYNOPSIS GRAPHIC

